resulted in extracellular synthesis. As a part of our ongoing investigations into fungus-based biotransformation synthesis protocols for nanoparticles, we present herein details of synthesis of silver nanoparticles both intra- and extracellularly using *Verticillium* and *Fusarium oxysporum* respectively. The reduction of Ag^+ ions by these fungi suggest the release of fairly strong reducing agents and adds considerably to the range of applicability of our fungal-based synthesis protocol. We believe that the intracellular synthesis of silver nanoparticles by the fungus occurs by the reductases present in the fungal cell wall while the extracellular synthesis occurs through the release of reductases into solution.

2. Experimental

2.1. Biosynthesis of silver nanoparticles using fungi :

2.1.1. Intracellular synthesis of silver nanoparticles using Verticillium sp.

The fungus, *Verticillium* sp. was isolated from the *Taxus* plant and preserved on potato-dextrose agar (PDA) slants at 25°C. The fungus was grown in 100 mL MGYP media, composed of glucose (1.0%), malt extract (0.3%), yeast extract (0.3%), and peptone (0.5%) at 24–27°C under shaking condition at 200 rpm for 4 days. After completion of fermentation, mycelial mass were separated from the culture broth by centrifugation (5000 rpm) at 10–15°C for 15 min and again washed twice with sterile distilled water. The settled mycelial mass was then re-suspended in 100 mL sterile distilled water in 500 mL conical flask and to this suspension, an aqueous solution of 10^{-4} M silver nitrate ($AgNO_3$) was added. The whole mixture was thereafter put into a shaker at 25–28°C (200 rpm) and the reaction was carried out for a period of 72 h. The biotransformation was routinely monitored by visual inspection of the biomass as well as measurement of the UV-Vis spectra from the fungal cells.

2.1.2. Extracellular synthesis of silver nanoparticles using Fusarium oxysporum

The fungus, *Fusarium oxysporum* (*F. oxysporum* f.sp.*ciceri* NCIM1282) was maintained on potato-dextrose agar (PDA) slants at 25°C. The procedure for growing and washing the fungus was identical to that described earlier for the intracellular synthesis of silver nanoparticles by *Verticillium* and for brevity, will not be repeated here. The settled mycelial mass thus obtained after washing was resuspended in 100 mL of 10^{-3} M aqueous $AgNO_3$ solution in 500 mL conical flasks. The whole mixture was put into a shaker at 25–28°C (200 rpm). The biotransformation was routinely monitored by periodic sampling of aliquots (2 mL) of the aqueous component and measuring the UV-Vis spectra of the solution.

2.2. Characterization :

Films of the fungal cells for UV-Vis spectroscopy and X-ray diffraction (XRD) studies were prepared by solution casting onto Si(111) wafers and thoroughly drying the film in flowing N_2. XRD patterns of the nano Ag-fungal cells were recorded on a Rigaku D Max III VC instrument with Ni filtered Cu K_α radiation (λ = 1.5404 Å) in the 2θ range of 30–80° at a scan rate of 2°/min. UV-Vis spectroscopic measurements of the films as well as the solutions were made on a Shimadzu dual-beam spectrophotometer (model UV-1601PC) operating in the reflection mode at a resolution of 2 nm. FTIR studies were carried out on a Shimadzu FTIR-8201PC instrument in the diffuse reflectance mode at a resolution of 4 cm^{-1} after drop coating the solution on a Si wafer. Transmission electron microscopy (TEM) studies of thin sections of the nano-Ag-*Verticillium* cells and the nano Ag solution were carried out on a JEOL Model 1200EX instrument operated at an accelerating voltage of 60 kV. The procedure for preparation of the nano-Ag-*Verticillium* cells was identical to that used earlier in the study of nano-Au-*Verticillium* fungal cells [21] and for brevity, will not be repeated again.

3. Results and discussion

3.1. Intracellular synthesis :

3.1.1. By visual inspection

Figure 1A shows two conical flasks of the *Verticillium* fungal biomass before (1) and after (2) exposure to 10^{-4} M $AgNO_3$ solution. The pale yellow color of the biomass before the reaction (1) with Ag^+ ions can clearly be seen which changes to dark brown color after the completion of reaction (2). The appearance of dark brown color in the fungal biomass after the reaction indicates of intracellular synthesis of silver nanoparticles.

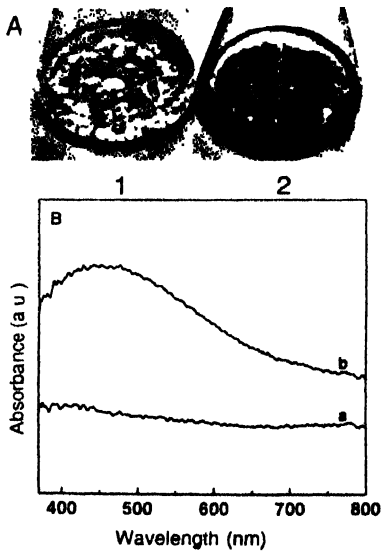

Figure 1. (A) Picture of two conical flasks containing the *Verticillium* fungal cells after removal from the culture media (1) and after immersion of *Verticillium* fungal cells in 10^{-4} M $AgNO_3$ soluion for 72 h (2). (B) UV-Vis spectra recorded from biofilms of the *Verticillium* fungal cells before (curve a) and after exposure to 10^{-4} M aqueous $AgNO_3$ solution for 72 h (curve b).

3.1.2. Optical properties

It is well known that silver nanoparticles absorb radiation in the visible region of the electromagnetic spectrum (*ca.* 380–450 nm)

due to excitation of surface plasmon resonance [23,24]. Figure 1B shows the UV-Vis spectra recorded from a film of the fungal cells before (curve a) and after immersion in 10^{-4} M $AgNO_3$ solution for 72 h (curve b). There is no evidence of absorption in the spectral window 400–800 nm in the case of the as-harvested fungal cells, while the fungal cells exposed to Ag^+ ions show a distinct and fairly broad absorption band centered at *ca.* 450 nm. The presence of the broad resonance indicates an aggregated structure of the silver particles in the film. The scattering from the rough fungal biomass surface would also contribute to the broadening of the resonance. The wavelength of the resonance is close to that observed for thin films of silver nanoparticles complexed with fatty lipid lamellae in Langmuir-Blodgett films [25] as well as in thermally evaporated lipid matrices [26].

3.1.3. X-ray diffraction

The further characterization for the intracellular synthesis of silver nanoparticles is provided by X-ray diffraction (XRD) analysis of the nano-Ag-*Verticillium* biofilm deposited on a Si wafer and is shown in Figure 2. The presence of intense peaks corresponding to the (111), (200) and (220) Bragg reflections of silver (identified in the diffraction pattern) agree well with those reported for silver nanocrystals [27]. The mean size of the silver nanoparticles formed in the cells was calculated by using the Debye-Scherrer equation by determining the width of the (111) Bragg reflection [28], and was found to be 30 nm.

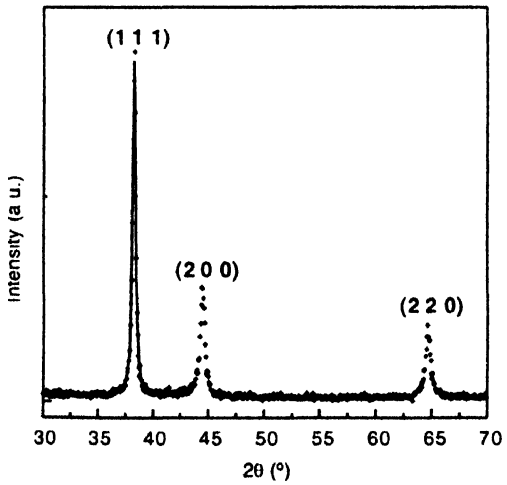

Figure 2. (B) XRD pattern recorded from an Au nano-*Verticillium* biofilm formed on a Si (111) wafer. The principal Bragg reflections are identified The solid line is a Lorentzian fit to the data and has been used to estimate the silver nanoparticle size.

3.1.4. Transmission Electron Microscopy

In order to understand the mechanism of formation of the silver nanoparticles in the biofilm, information on the position of the silver nanoparticles relative to the fungal cells is important. This was easily done by TEM analysis of thin sections of the nano-Ag-*Verticillium* cells, images of which are shown at various magnifications in Figure 3. At lower magnification, a number of *Verticillium* cells can be seen in Figure 3A. On careful inspection of the image, small particles of silver organized on the cell walls as well as some larger particles although considerably less in number was observed within the cells. Figure 3B shows TEM image of a single *Verticillium* cell in which silver nanoparticles both on the cell wall (outer boundary) as well as on the cytoplasmic membrane (inner boundary) was observed. The density of silver nanoparticles is clearly higher on the cytoplasmic membrane than on the cell wall. Selected area electron diffraction analysis of a single silver particle (data not shown) revealed diffuse rings with lattice spacings in excellent agreement with those reported for silver nanocrystals. A statistical analysis of the size of silver nanoparticles from many TEM images of single *Verticillium* cells resulted in an average silver nanoparticle size of 25 ± 8 nm. Higher magnification TEM image of one of the cells in Figure 3C shows highly organized assembly of silver nanoparticles on the membrane. A number of silver particles are observed that are spherical in morphology.

Figure 3. TEM images at different magnifications (A-C) of thin sections of stained *Verticillium* cells after reaction with $AgNO_3$ ions for 72 h

3.1.5. Probable mechanism

While the exact mechanism of formation of silver nanoparticles by reaction with the fungal cells is not clearly understood, but based on the results presented above we speculate the following. Since the nanoparticles are formed on the surface of the fungal biomass and not in solution, we believe that the first step is the trapping of the Ag^+ ions on the surface of the fungal cells *via* electrostatic interaction between the positively charged Ag^+ and negatively charged carboxylate groups in enzymes present in the cell wall of the biomass. Thereafter, the enzymes present in the cell wall reduce silver ions and lead to the formation of silver nanoparticles. The TEM results indicate the presence of some silver nanoparticles on the cytoplasmic membrane as well as within the cytoplasm (Figure 3C). This can be explained by considering that some Ag^+ ions may pass through the cell wall and reduced by enzymes present itself on the cytoplasmic membrane or within the cytoplasm. It may also be possible that some of the smaller silver nanoparticles diffuse across the cell wall and trapped within the cytoplasm. A more detailed structural study of the nano-Ag-*Verticillium* cells is necessary to understand the exact mechanism of silver nanoparticle formation.

3.2. Extracellular synthesis :

3.2.1. By visual inspection

Figure 4A shows two conical flasks with the *Fusarium*

oxysporum biomass before (1) and after (2) reaction with an aqueous solution of 10^{-3} M $AgNO_3$ for 72 h. It is observed that the biomass has a pale yellow color before reaction with the silver ions (1), which changes to a brownish color on completion of the reaction (2). The appearance of a yellowish-brown color in solution containing the biomass is a clear indication of the formation of silver nanoparticles in the reaction mixture and is due to excitation of surface plasmon vibrations in the nanoparticles [23,24]. Upon filtration, it was observed that the color of the aqueous solution was brown which clearly indicates the extracellular reduction of the Ag^+ ions.

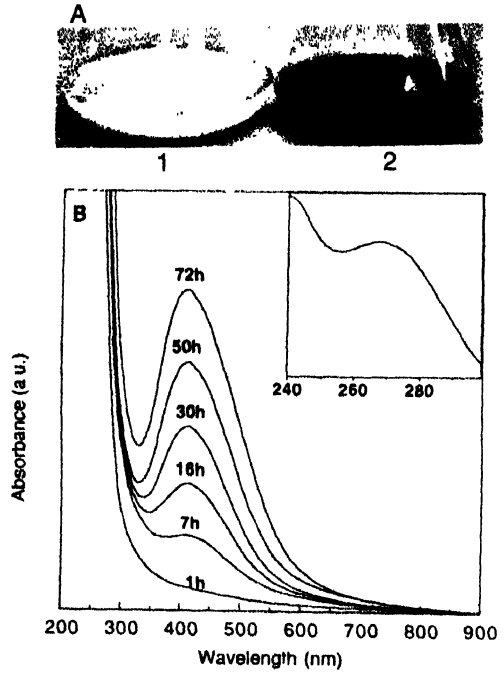

Figure 4. (A) Picture of conical flasks containing the *Fusarium oxysporum* biomass before removal from the culture media (1) and after immersion in 10^{-3} M $AgNO_3$ solution (2). (B) UV-Vis spectra recorded as a function of time of reaction of an aqueous solution of 10^{-3} M $AgNO_3$ with the fungal biomass. The time of reaction is indicated next to the respective curve. The inset shows the UV-Vis absorption spectrum in the low wavelength region recorded from the reaction medium 72 h after commencement of reaction.

3.2.2. Optical properties

Figure 4B shows the UV-Vis spectra recorded from the *Fusarium oxysporum* reaction vessel at different interval of time. The strong surface plasmon resonance centered at *ca.* 415 nm also suggests the formation of silver nanoparticles. The plasmon resonance is sharp and indicates little aggregation of the particles in solution. Quite interestingly, Ag nanoparticle solutions were extremely stable with no evidence of aggregation of the particles even after a month of reaction. The inset of Figure 4B shows the UV-Vis spectrum in the low wavelength region recorded from the $AgNO_3$ reaction medium after 72 h of reaction. The appearance of absorption band at *ca.* 280 nm clearly indicates the release of proteins [29] into solution by *Fusarium oxysporum* and a possible mechanism for the reduction of the metal ions. These proteins are also believed to stabilize the particles against aggregation by binding to their surface.

3.2.3. FTIR measurements

FTIR measurements carried out on a drop-coated film of the silver nanoparticle fungus reaction solution after 72 h showed the presence of three bands at 1650 cm^{-1} (1), 1540 cm^{-1} (2) and 1450 cm^{-1} (3) in Figure 5A. The bands at 1650 and 1540 cm^{-1} are identified as the amide I and II bands and arise due to carbonyl stretch and -NH stretch vibrations present in the amide linkages of the proteins, respectively. The positions of these bands are close to that reported for native proteins [30–34]. The FTIR results thus indicate that the secondary structure of the proteins is not affected as a consequence of reaction with the Ag^+ ions or binding with the silver nanoparticles. The band at *ca.* 1450 cm^{-1} is assigned to ethylene scissoring vibrations from the proteins in the solution.

3.2.4. Transmission Electron Microscopic experiments

A representative TEM image recorded from the silver nanoparticles film deposited on a carbon-coated copper TEM grid is shown in Figure 5B and shows individual silver particles as well as a number of aggregates. Under observation of this image in an optical microscope, it was found that the morphology of the nanoparticles is highly variable, with spherical and occasionally triangular nanoparticles. These particles have a size range of 5–50 nm.

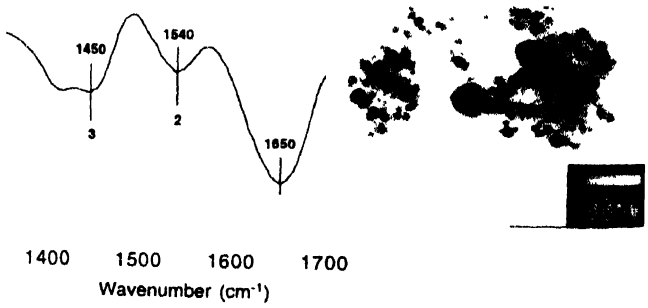

Figure 5. (A) FTIR spectrum recorded from a drop-coated film of an aqueous solution incubated with *Fusarium oxysporum* and reacted with Ag^+ ions for 72 h. (B) TEM micrograph recorded from a drop-coated film of aqueous silver nanoparticle solution.

3.2.5. Probable mechanism

In order to understand the exact mechanism of reduction of silver ions in solution, the following experiment was performed. 10 g of the biomass was immersed in 100 ml of water for 72 h at 200 rpm and then separated by filtration. To this filtrate, 10^{-3} M $AgNO_3$ was added. It was observed that this initially colorless aqueous solution changed to a pale yellowish-brown within 24 h of reaction (not shown), clearly indicating that the *Fusarium oxysporum* releases reducing agents into solution that are responsible for formation of the silver nanoparticles. As this

experiment clearly establishes that the reduction of the Ag^+ ions occurs extracellularly, it would be important to identify the reducing agents responsible for this. A preliminary gel electrophoresis study of the aqueous solution (not shown) indicates the presence of a minimum of four high molecular weight proteins released by the biomass. Preliminary protein assay indicates that one of the proteins was an NADH-dependent reductase. We believe this reductase is responsible for the reduction of Ag^+ ions and the subsequent formation of silver nanoparticles. The long-term stability of the nanoparticle solution mentioned earlier may be due to the stabilization of the silver particles by the proteins. Silver nanoparticles have been reported to interact strongly with enzymes such as cytochrome C [30,31] and a similar binding mechanism may be operative in this study.

4. Conclusion

To conclude, we have demonstrated the intra- and extracellular formation of silver nanoparticles using appropriate genera of fungi, *Verticillium* sp. and *Fusarium oxysporum* respectively. In case of intracellular synthesis, the reduction of novel metal ions occurs by the reductase enzyme present on the surface of the mycelia as well as on the cytoplasmic membrane and these surface bound nanoparticles may be used in catalysis and as precursors for synthesis of coatings for electronic applications. The extracellular synthesis of nanoparticles is exciting as these may be used in homogeneous catalysis, the nanoparticles may be immobilized in different matrices or in thin-film form for optoelectronic applications. This fungal mediated environmentally friendly "green chemical" approach towards the synthesis of nanoparticles has many advantages, such as the ease with which the process can be scaled up, economic viability *etc*. The shift from bacteria to fungi as a means of developing natural "nanofactories" has the added advantage that processing and handling of the biomass would be much simpler. Further, compared to bacteria, fungi are known to secrete much higher amounts of proteins, thereby significantly increasing the productivity of this biosynthetic approach.

Acknowledgments

SS and DM gratefully acknowledge the Council of Scientific and Industrial Research, New Delhi, Government of India, for grant of research fellowships. We thank Dr. P Mukherjee for helpful discussions.

References

[1] K Simkiss and K M Wilbur *Biomineralization* (New York : Academic) (1989)

[2] S Mann (ed.) *Biomimetic Materials Chemistry* (Weinheim : VCH) (1996)

[3] D R Loveley, J F Stolz, G L Nord and E J P Phillips *Nature* **330** 252 (1987)

[4] D P E Dickson *J Magn. Magn. Mater.* **203** 46 (1999)

[5] S Mann *Nature* **365** 499 (1993)

[6] S Oliver, A Kupermann, N Coombs, A Lough and G A Ozin *Nature* **378** 47 (1995)

[7] N Kroger, R Deutzmann and M Sumper *Science* **286** 1129 (1999)

[8] D Pum and U B Sleytr *Trends Biotechnol* **17** 8 (1999)

[9] U B Sleytr, P Messner, D Pum and M Sara *Angew. Chem. Int. Ed* **38** 1034 (1999)

[10] J R Stephen and S J Maenaughton *Curr Opin Biotechnol.* **10** 230 (1999)

[11] R K Mehra and D R Winge *J. Cell. Biochem.* **45** 30 (1991)

[12] G Southam and T J Beveridge *Geochim Cosmochim Acta* **60** 4369 (1996)

[13] T J Beveridge and R G E Murray *J. Bacteriol* **141** 876 (1980)

[14] D Fortin and T J Beveridge in *Biomineralization. From Biology to Biotechnology and Medical Applications* (ed) E. Baeuerlen, Wiley-VCH, Weinheim p7 (2000)

[15] T Klaus, R Joerger, E Olsson and C G Granqvist *Proc. Natl. Acad Sci* **96** 13611 (1999)

[16] T Klaus-Joerger, R Joerger, E Olsson and C G Granqvist *Trends Biotechnol* **19** 15 (2001)

[17] R Joerger, T Klaus and C G Granqvist *Adv. Mater.* **12** 407 (2000)

[18] B Nair and T Pradeep *Crys. Growth & Design* **2** 293 (2002)

[19] J L Gardea-Torresdey, J G Parsons, E Gomez, J Peralta-Videa, H E Troiani, P Santiago and M Jose-Yacaman *Nano Lett.* **2** 397 (2002)

[20] J L Gardea-Torresdey, E Gomez, J Peralta-Videa, J G Parsons, H E Troiani and M Jose-Yacaman *Langmuir* (2003) in press

[21] P Mukherjee, A Ahmad, D Mandal, S Senapati, S R Sainkar, M I Khan, R Ramani, R Parischa, P V Ajaykumar, M Alam, M Sastry and R Kumar *Angew. Chem. Int. Ed* **40** 3585 (2001)

[22] P Mukherjee, S Senapati, D Mandal, A Ahmad, M I Khan, R Kumar and M Sastry *Chem. Bio. Chem* **3** 461 (2002)

[23] A Henglein *J Phys. Chem* **97** 5467 (1993)

[24] M Sastry, K Bandyopadhyay and K S Mayya *Coll Surf* **A127** 221 (1997)

[25] M Sastry, K S Mayya, V Patil, D V Paranjape and S G Hegde *J Phys Chem* **B101** 4954 (1997)

[26] M Sastry, V Patil and S R Sainkar *J Phys. Chem.* **B102** 1404 (1998)

[27] D V Leff, L Brandt and J R Heath *Langmuir* **12** 4723 (1996)

[28] J W Jeffrey *Methods in Crystallography* (New York · Academic) (1971)

[29] Cantor and Schimmel *Biophysical Chemistry, Part II Techniques for the Study of Biological Structure and Function* Ch7 p377 (1980)

[30] I D G Macdonald and W E Smith *Langmuir* **12** 706 (1996)

[31] C D Keating, K K Kovaleski and M J Natan *J. Phys Chem* **B102** 9414 (1998)

[32] A Gole, C Dash, V Ramakrishnan, S R Sainkar, A B Mandale, M Rao and M Sastry *Langmuir* **17** 1674 (2001) (and references therein)

[33] C V Kumar and G L McLendon *Chem. Mater.* **9** 863 (1997)

[34] A Gole, C Dash, S R Sainkar, A B Mandale, M Rao and M Sastry *Anal. Chem.* **72** 1401 (2000)